IEEE Robotics and Automation Letters (RA-L) paper, presented at ICRA 2024, Yokohama, Japan. Cite as RA-L paper.

Design and Analysis of Adaptive Flipper with Origami Structure for Frog-inspired Swimming Robot

Shuqi Wang, Jizhuang Fan, *Member, IEEE*, Yitao Pan, Gangfeng Liu, *Member, IEEE*, Yubin Liu

***Abstract*—Flippers are important components for improving the locomotion efficiency and stability of bionic underwater robots. A novel origami-based adaptive flipper is presented to address a lack of environmental adaptability and low performance efficiency due to the structural design or inherent characteristics of its main constituent materials. The design decision process and locomotion principle of the flipper are introduced in detail. It can exhibit better adaptive deformation under the action of hydrodynamics without affecting the propulsion efficiency. Kinematics and simulation analysis are performed to characterize the influence of structural parameters on the motion performance. Experimental swimming results show that compared with ordinary flippers, the locomotion efficiency is greatly improved with the help of origami flippers. The origami flipper also shows good adaptability when in contact with the external environment and overcomes the inability of open-close flippers to cross a 90° corner, which shows the rationality of the structural design and the feasibility of its application in underwater robots.**

***Index Terms*—Flippers, origami structure, adaptability, locomotion efficiency.**

I. Introduction

As carriers of detection and communication equipment, underwater robots play an increasingly important role in the fields of marine resource exploration and environmental monitoring. Different forms of bionic swimming robots have been successfully developed.[1–3] The propulsion methods adopted by most robots mainly include propeller propulsion, caudal fin propulsion, middle fin propulsion and recoil propulsion.[4–6] Although the above propulsion methods can provide movement, the propulsion efficiency, flexibility and stability need to be improved.[7] The unknown underwater environment also place higher requirements on the locomotion mode and structural stability of the robot. A frog can swim smoothly and quickly by using the flipper stroke method, which provides a new idea for research on the propulsion structure of bionic swimming robots.[8,9] The propulsive mode of the flipper stroke has obvious advantages in propulsive efficiency, mobility and stability, as shown in Table I.

However, as a main driving unit for bionic swimming robots, few studies have focused on the design of flipper structures for improving locomotion efficiency. The design of flippers is mainly attached to the research of frog-inspired robots, which is not a key research object.[10–12] The design is often simplified into a hard plate structure[13–15], which cannot adjust the flipper structure automatically according to the locomotion form to reduce water resistance, resulting in low locomotion efficiency.

To solve the problems faced by hard flippers, some solutions have been proposed in combination with novel materials and technologies. A folding principle similar to that of a fan has been adopted in an active flipper.[16,17] One side of the flipper is fixed, and the other side is driven by the rotation of a waterproof steering gear to realize the opening and closing movement.[18] Silica gel material has been introduced into flipper design, which has a certain flexibility while ensuring sufficient strength.[19] However, the flipper also needs to be driven by external units, resulting in a more complex structure and heavier robot weight.[20] On this basis, a passive flipper with a sliding module is proposed. The flipper has four toes that are all four-bar linkages, which can increase the angle of attack on water to increase the contact area by following the translation of the lateral tarsal bone. In addition, a force spring and a strain gauge are added to complete the measurement of the flipper force. Although the passive flipper structure has been improved, there are still shortcomings, such as large volume and heavy weight, which lead to poor environmental adaptability and flexibility.[21] Meanwhile, the toes of these flippers are made of rigid materials, which are prone to collision damage when in contact with external obstacles. In view of the shortcomings of current bionic flippers, which are mainly made of rigid materials or have low structural adaptability, there is no bionic flipper designed to simulate a frog's swimming mode. Therefore, it is important to develop a small and lightweight bionic flipper based on biological characteristics to improve the locomotion performance of frog-inspired swimming robots.

The field of rigid foldable origami is an active area of research.[22–24] The origami-inspired folding of deployable

Manuscript received: 3 July 2023; Revised 30 August 2023; Accepted 9 November 2023. This paper was recommended for publication by Editor X. Liu upon evaluation of the Associate Editor and Reviewers' comments. This work was supported by National Natural Science Foundation of China (Grant No. 51675124). (Corresponding author: Yubin Liu).

The authors are with the State Key Laboratory of Robotics and System, Harbin Institute of Technology, Harbin 150001, Heilongjiang, China (e-mail: wangshuqi@hit.edu.cn; fanjizhuang@hit.edu.cn; 21b308005@stu.hit.edu.cn; liugangfeng@hit.edu.cn; liuyubin@hit.edu.cn).

Digital Object Identifier (DOI): see top of this page.

IEEE Robotics and Automation Letters (RA-L) paper, presented at ICRA 2024, Yokohama, Japan. Cite as RA-L paper.

systems can achieve a compact storage volume during launch and flight that will be deployed into a much larger volume when the target location is reached.[25–27] Therefore, researchers have gradually carried out in-depth research on this topic in recent years and have achieved some remarkable results in the research of soft materials and the design of robot structures.[28–31] The types and numbers of robots based on origami structures have been increasing.[32–34] The simple structure and high adaptability of origami can better solve the problems faced by the abovementioned flippers.[35] In this regard, an adaptive flipper with a large shrinkage rate based on an origami structure is proposed, which can show different shapes under the action of hydrodynamics according to different motion forms. Notably, it does not require the robot to provide any power to change the structural shape, such as steering gear or an air source, which simplifies the robot mechanism and improves the locomotion efficiency. Meanwhile, the folding structure also enhances the adaptability of the robot to the external environment.

TABLE I. COMPARISON OF DIFFERENT SWIMMING MODES

Content	The way of swimming			
	Caudal fin advance	***Mid-fin propulsion***	***Recoil***	***Flippers***
Propulsion mechanism	The wave or swing of the tail fin and the body to form a forward thrust	Pairs of fins, flapping or waves to advance	The cavity absorbs and discharges water to advance	Periodic limb swing to advance and adjust posture
Speed	High	Low	Low	High
Efficiency	High	High	Low	High
Flexibility	Low	High	Low	High
Stability	Low	High	Low	High

In the following section, the design principle and preparation of bionic flippers are proposed based on an analysis of a frog's flipper structure and its locomotion characteristics. Subsequently, the modeling and simulation analysis of the flipper are carried out combined with the locomotion principle in Section 3, and an analysis related to the choice of the best flipper design is also described. In the Experimental Analysis section, experiments verifying the rationality and feasibility of the design of the flipper structure are shown. Finally, a discussion of the results is provided.

II. DESIGN AND PROPERTIES OF THE PROPOSED FLIPPER

A. Analysis of biological characteristics

A frog can freely adjust its movement posture with its strong hind limbs to complete forward, turning and diving motions in water. The skeletal structure of a hind limb and its flippers are shown in Fig. 1a. The foot bone is composed of a chain of flexible toes formed by the tarsal bone and five phalanges. The feet are long and flexible and have webbing between the toes. The tarsal bone forms a hollow arched foot with inward depression. From the perspective of mechanics, the torso will be subjected to gravity from the tibia to the tarsal bone. The force is applied to the entire foot because the tarsal bone is arched so that the frog's torso is in a relatively stable state.

The swimming process of frogs can be obtained by movement observation experiments,[9] which are composed of three main movement stages: propulsion, sliding and recovery. The movement diagram of the hind limbs and flippers during the stroke is shown in Fig. 1b. The flipper starts to open from the initial moment of the propulsion stage and fully opens when the tarsometatarsal joint is open, which increases the contact area with water. Meanwhile, the leg stretches rapidly so that it can produce greater propulsion force during the propulsion process. The whole propulsion motion is an outer arc motion. The hind limbs remained basically immobile during the sliding phase until the recovery phase, while the flippers remain contracted to reduce resistance. In the recovery stage, the movement is relatively slow, and the hind limbs begin to contract slowly. The contraction of the ankle joint is generally later than the movement of the leg, so most of the flippers are hidden behind the thigh, while the flippers maintain the contraction state at this time to reduce the contact area with water. Notably, the flippers can float backward with the water flow to greatly reduce the recovery resistance because of their flexible characteristics. The whole recovery movement is in the inner arc.

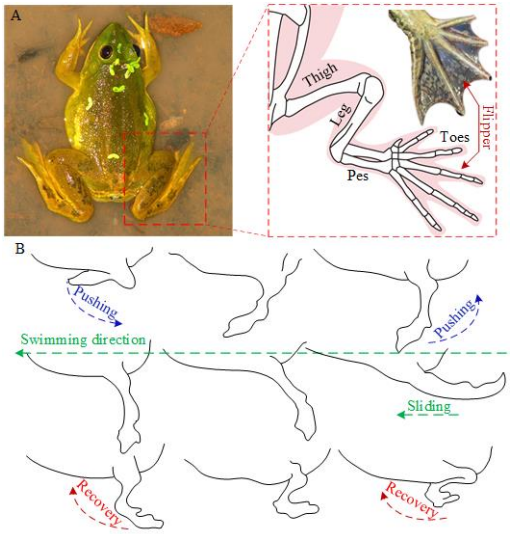

Fig. 1. The biological structure and movement characteristics of frogs. (A) The skeletal structure of the hind limb and its flipper. (B) The swimming sequence diagram of frog hind limbs.

B. Design and Prototyping

As an important component of the frog-inspired swimming robot, the flipper is the driving unit in the propulsion process, as well as one of the resistance sources in the recovery movement. The structure and adaptability of the flipper have a great influence on the locomotion efficiency of the robot. Adjusting the structure according to different stages is the key to meet the motion requirements and improve the motion efficiency of the robot. Referring to the artistic origami shown in Fig. 2a, a 2D schematic diagram of an origami flipper is designed, as shown in Fig. 2b. The solid line represents the peak line, that is, the crease protrusion, and the dotted line is the opposite, representing the valley line.

The origami-based adaptive flipper is mainly composed of N groups of deformable folding units U, where N is an integer

greater than or equal to 1. Each unit contains two moving flippers, two rows of fixed flippers arranged in a gradually increasing manner from the proximal to the distal end, and multiple deformation limiting blocks. The fixed flipper at the proximal end is arranged with a moving flipper that swings unidirectionally and is placed on the forced side of the propulsion motion so that the one-way drainage mechanism can be generated during the recovery motion to reduce resistance and improve recovery efficiency without affecting propulsion efficiency. The transverse creases in each row of the flippers and the longitudinal creases between the adjacent two rows of the flippers are alternately set from proximal to distal as the peak line and the valley line. Notably, the longitudinal crease between the adjacent two units is opposite, which is alternately set by the valley line and the peak line, so that the shape of the flipper after the expansion is fan-shaped and fits the biological characteristics.

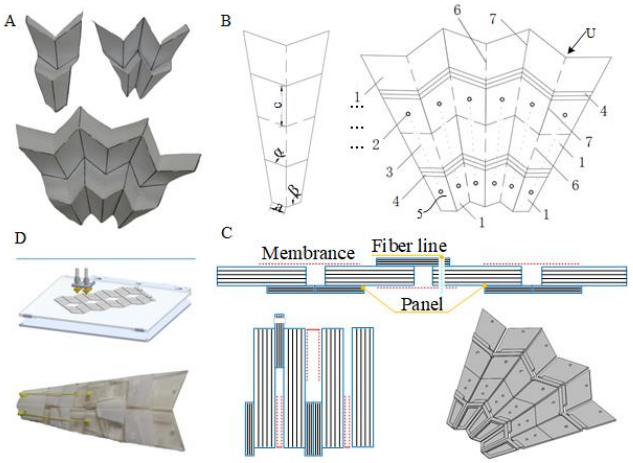

Fig. 2. Steps of the proposed approach for the design, modeling and preparation of a bionic flipper according to artistic origami. (A) Concept: artistic origami. (B) Modeling: origami unit folds and tessellation. (C) Design: skeleton and its folded design. (D) Fabrication: printing and adhesion.

Furthermore, the deformation limit blocks are arranged transversely at the peak line of the fixed flippers in the unit or between the units, as shown in the design section of Fig. 2c, so that they can be closed and squeezed to produce force after the flipper is expanded, thereby improving the structural strength of the flipper to prevent excessive deformation. This arrangement on the peak line will not affect the degree of contraction of the flipper. In addition, each unit contains two limit lines, which are set on the forced side of the flipper during the propulsion process. The positioning hole is set on the odd fixed flipper from the proximal end, and the limit line connects the two fixed flippers across the deformation limit block and the peak line to prevent the middle of the flipper from shrinking along the valley line due to the force on the distal end to ensure sufficient force contact area. The radial length and expansion area of the flipper can be flexibly adjusted by increasing the number of fixed flippers or the number of units A to adapt to different working requirements.

C. Preparation and locomotion principle

It can be seen that the flipper structure is a very simple design concept, and primarily composed of movable and fixed flippers; the materials used are readily available and purchased from commercial companies. The deformation limit block and the fixed flipper are designed as a whole, both of which are made of lighter 8000 resin materials and processed by 3D printing, which is convenient for processing, manufacturing and assembly. The movable flipper is cut and formed by a PVC transparent plastic plate with a material thickness of 0.2 mm and is connected with the fixed flipper only by the bonding at proximal end, which can produce the effect of unidirectional drainage. The peak line and valley line between adjacent fixed flippers are flexibly bonded and connected by lightweight and non-stretchable materials, creating a form of motion that rotates only around the crease with only one rotational degree of freedom. In this way, the force on the proximal flipper during the recovery movement will gradually transfer to the distal end to promote the contraction of the flipper, and vice versa. A Kevlar fiber line with high strength and light weight is used as the limit line. Therefore, the flipper has the characteristics of rigidity, softness and flexibility combined with reasonable material selection. The flexible connection can also promote the adaptive deformation of the flipper in contact with the external rigid body to avoid collision damage and enhance its adaptability to the external environment.

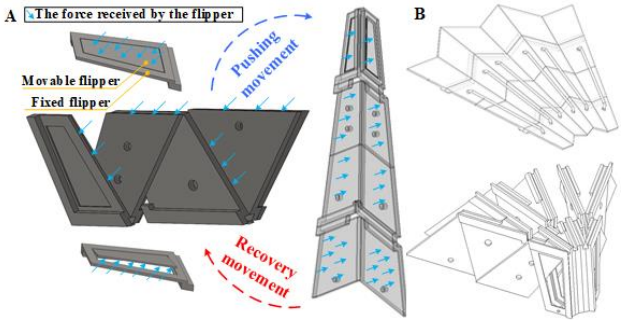

Fig. 3. The locomotion principle of the bionic flipper. (A) The force diagram of the flipper under different motion states. The movable flipper can produce a unidirectional drainage mechanism to improve the movement efficiency. (B) Initial and contraction states of the multiunit flippers.

Since the movement of the flipper is directional, it is very important to first clarify its front and back. The state shown in Fig. 3a is taken as the front, that is, the forced surface during the recovery motion. The natural floating of the flipper in the water is taken as its initial state, and the movable flipper is placed on the force side of the propulsion motion. The water exerts force on the valley line when the flipper begins to move and drives it to start stretching along the crease. The water resistance increases with increasing speed, and the opening area of the flipper also increases gradually, which further increases the contact area with water. These factors are positively correlated and promote each other. The limit line begins to tighten to prevent the distal end from shrinking along the valley line when the flipper is fully expanded. Meanwhile, the deformation limit block at the peak line begins to close and squeeze, and force is generated to ensure that the flipper does not produce excessive deformation when subjected to a large medium force. The reaction force of the flipper in full contact with the water can be

IEEE Robotics and Automation Letters (RA-L) paper, presented at ICRA 2024, Yokohama, Japan. Cite as RA-L paper.

used as the main power source to realize the propulsion motion of the robot.

The deformed limit block and limit line instantaneously lose the limit effect at the beginning of the recovery motion, and the flippers are only subjected to the force of the water. The force is mainly concentrated at the valley line because the peak line has a certain diversion effect, and the valley line begins to shrink horizontally and vertically after being forced. The contraction force generated by the proximal end will also be transmitted to the entire flipper by a flexible material that is not stretchable due to wavy transverse creases, so each unit shrinks along the crease to drive the entire flipper to achieve autonomous contraction. With the help of the deformation limit block and the limit line, the adaptive deformation can be carried out according to the designed crease path only by relying on the resistance of the water; that is, the extension and recovery of the flipper are changed with the motion state. Without providing power or a driving device, the structure of the robot is simplified, and the motion efficiency is improved. To further highlight the superiority of origami flippers, we made a comparison with traditional flippers, as shown in Table II. It can be seen that the use of an origami structure and soft materials changes its driving mode, which not only reduces the weight and size but also improves its scalability.

TABLE II. COMPARISON OF DIFFERENT FLIPPERS

Content	The properties of flippers				
	Weight	***Size***	***Scalability***	***Material***	***Driven***
Traditional flippers	Heavy	Big	Poor	Hard	Motor
Origami flippers	Light	Small	Good	Hard and soft	Water

III. MODELING AND ANALYSIS

A. Deformation model analysis

The contraction degree of the flipper during the recovery process has a great influence on the locomotion efficiency, so the change in the forced area during the movement is a key point of the proposed flipper. To analyze the influence of its structural parameters on the shrinkage rate, the theoretical model of such changes is provided in the following. A deformed structural model is shown in Fig. 4.

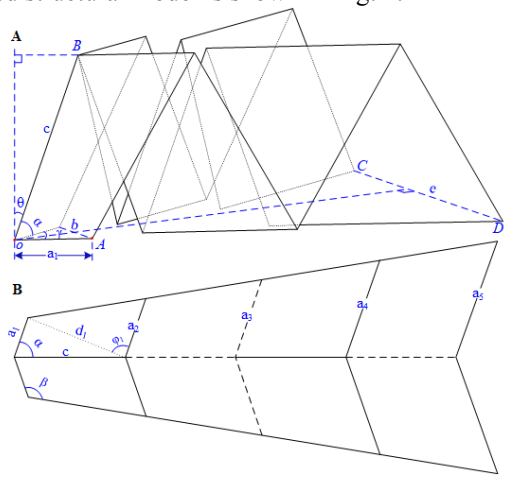

Fig. 4. Deformation modeling. (A) Contraction state. (B) Fully stretched state.

The following assumptions are proposed to simplify analysis of the bionic flipper modeling process: (1) The area of the deformation limit block and the positioning hole on the fixed flipper is negligible for the overall area after it is fully expanded. (2) The flipper will not produce excessive deformation under the action of the external limit line, that is, the expanded flipper is a planar structure. (3) The flexible connecting material only plays the role of a hinge, that is, ignoring the influence of its stretching on the deformation process of the flipper. (4) The overall volume of the flipper remains unchanged during deformation.

The force area of the contracted flipper is S_C when the folding angle of the proximal fixed flipper is γ. The area of the expanded flipper is S_E, where the ratio I_C of the two areas is defined as the shrinkage of the flipper:

$$I_C = 1 - \frac{S_C}{S_E}, I_C \in [0,1) \tag{1}$$

The shrinkage of the flipper can be taken as 0 when it is an unfoldable plate structure, and it is impossible to reach 1 due to its thickness. The force area during recovery motion can be expressed as:

$$S_C = \frac{\left(a_1^2 - a_n^2\right)}{2}\sin\gamma + \left(a_1 + a_n\right)\left(n\sin\theta + \left(a_n - a_1\right)\cos\frac{\gamma}{2}\right)\sin\frac{\gamma}{2} \tag{2}$$

where θ is the angle between the vertical direction and the first proximal flipper, which is related to the degree of contraction.

$$\theta = \arcsin\frac{(a_1 - a_2)\sin\beta}{c\sin\left(\beta + \gamma/2\right)} \tag{3}$$

Based on the expanded geometric relationship, the area of the flipper is expressed as:

$$S_E = \sum_{i=1}^{N} c\sin\alpha \times \left[a_i + c\sin\alpha\left(\frac{1}{\tan\varphi_i} - \frac{1}{\tan\beta}\right)\right] \tag{4}$$

where φ_i is the angle between the diagonal and the side of the fixed flipper, which can be written by the sinusoidal theorem:

$$\varphi_i = \arctan\left(\frac{c\sin\alpha}{a_i - c\cos\alpha}\right) \tag{5}$$

Based on the above analysis process, the relationship between the shrinkage rate I_C and the folding angle γ of the flipper is as follows:

$$I_C = 1 - \frac{\frac{\left(a_1^2 - a_n^2\right)}{2}\sin\gamma + \left(a_1 + a_n\right)\left(n\sin\theta + \left(a_n - a_1\right)\cos\frac{\gamma}{2}\right)\sin\frac{\gamma}{2}}{\sum_{i=1}^{n} c\sin\alpha \times \left[a_i + c\sin\alpha\left(\frac{a_i - c\cos\alpha}{c\sin\alpha} - \frac{1}{\tan\beta}\right)\right]} \tag{6}$$

The variables in the formula are related to the folding angle γ of the flipper.

B. Structural parameter analysis

Based on an analysis of the deformation model, the influence of structural parameters on shrinkage rate is studied more intuitively. The initial structural parameters $\{a_1, \beta\}$ of the

flipper are fixed due to the limitation of the overall size of the frog-inspired swimming robot. Combined with the deformation analysis model, the folding angle is mainly affected by the structural parameters $\{\alpha, c\}$. The expansion angle β=130° and the unilateral length a_1=15mm of the fixed flipper are controlled to explore the influence of different α and c values on the contraction characteristic curve of the flipper. As shown in Fig. 5, the larger α is, the greater the shrinkage of the flipper when the folding angle is the same; the larger c is, the larger the folding angle required to achieve the same shrinkage rate. The influence of the parameter $\{\alpha, c\}$ on the flipper can be intuitively recognized, but it cannot be used to accurately determine the final structural parameters of the flipper.

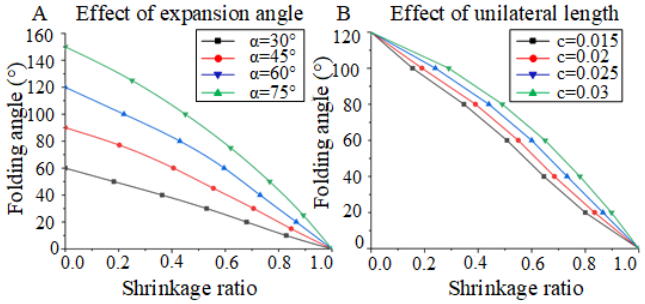

Fig. 5. The characteristic curve of the influence of structural parameters on flipper shrinkage. (A) Effect of the fixed flipper expansion angle on the shrinkage rate. (B) Effect of the fixed flipper unilateral length on the shrinkage rate.

C. Simulation analysis

The flipper not only needs to show the maximum shrinkage rate to reduce the recovery resistance, but also needs to have the largest drainage area to improve the propulsion efficiency. Therefore, the influence of structural parameters on the propulsion performance is further analyzed while ensuring the shrinkage rate, and the simulation motion analysis of the flipper is carried out in Fluent software. By using dynamic mesh technology, the flipper swing is controlled by user-defined function (UDF) programming to obtain the required flow field information. It can be assumed that the flipper is a non-thick surface because the influence of the thickness on the thrust is negligible, and the flipper baseline is a stationary baseline. A relatively long length is taken in the incoming flow direction, and a smaller length is taken in the other directions to reduce the amount of calculation. The calculated basin size is 600 × 4 mm × 200 mm in this study. Considering the balance between calculation accuracy and calculation time, the computational domain is divided into an inner domain using unstructured tetrahedral meshes to adapt to complex model features and an outer domain using structured meshes to save calculation time. The inlet boundary adopts the velocity boundary, and the outlet boundary adopts the pressure outlet. The time step is set to 0.0001 s, and the residual convergence condition is set to 1.0×10^{-5}.

The surface pressure cloud sequence of the flipper during propulsion is obtained by hydrodynamic simulation, as shown in Fig. 6a. During the propulsion process, the high-pressure center gradually moves to the distal end and tends to disappear, which can better drive the overall movement of the flipper. In addition, the pressure change at the distal end is much larger than that at the proximal end, so the swing at the proximal end has little effect on the propulsion performance, which preliminarily shows the rationality of the structural design of the narrow proximal end and wide distal end. From the pressure cloud diagram of different shapes in Fig. 6b, it can be seen that the surface pressure increases with increasing distal area, but the longitudinal length has a greater influence on the pressure than the area of the flipper. It can also be seen from the change in turbulence eddy dissipation in Fig. 6c that the dissipation coefficient is inversely proportional to the flow velocity. The increase in its value indicates that the heat transfer of turbulence increases, which makes the energy loss more serious and then affects the propulsion efficiency.

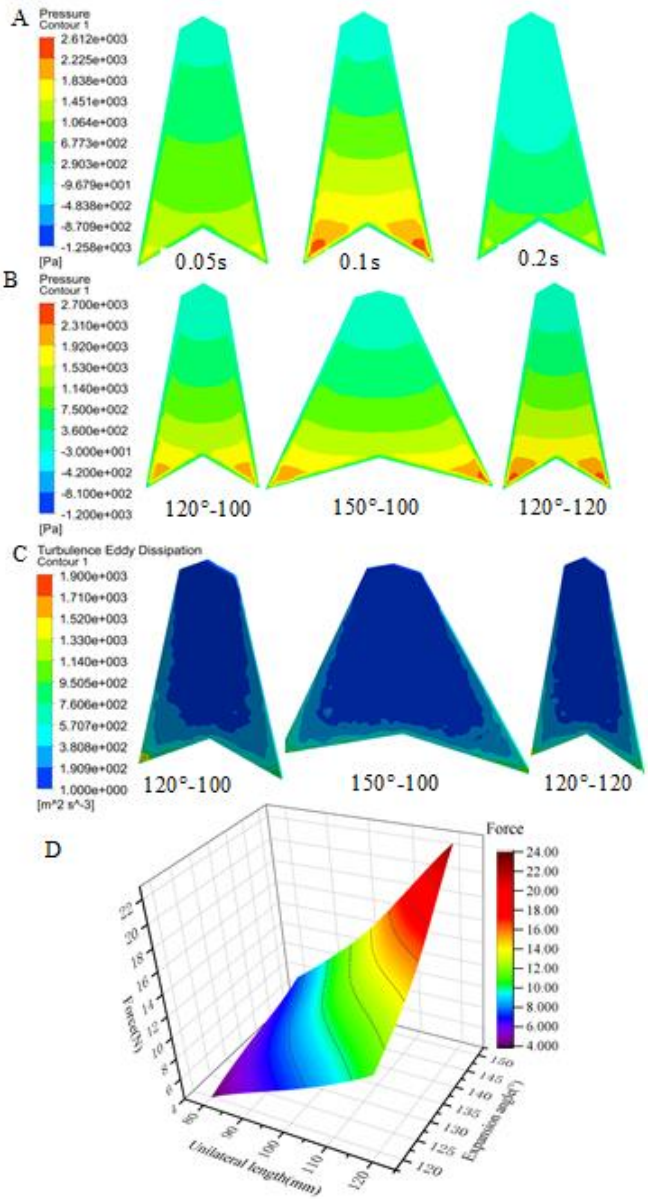

Fig. 6. The hydrodynamic simulation results of the flipper. (A) The pressure cloud diagram of the drainage surface at different times during the propulsion movement. (B) The pressure contours and (C) turbulence eddy dissipation of different structural parameters of the flipper. (D) The influence of structural parameters on the generated propulsion force.

IEEE Robotics and Automation Letters (RA-L) paper, presented at ICRA 2024, Yokohama, Japan. Cite as RA-L paper.

To more intuitively reflect the influence of shape on the motion performance, the maximum thrust generated is extracted to draw its change with the structural parameters. As shown in Fig. 6d, the propulsion force generated when the unilateral length is 120 mm is approximately three times that of 80 mm when the expansion angle is the same. When the unilateral length is the same, the propulsion force generated by the expansion angle of 150° is approximately twice that of 120°. Compared with the expansion angle, the unilateral length of the flipper also has a greater impact on the force. According to the above analysis, to ensure that the maximum thrust can be generated while ensuring the minimum area increase, the overall structural parameters of the bidirectional adaptive flipper are finally determined as shown in Table III (taking 4 segments as an example).

TABLE III. PARAMETERS OF THE ORIGAMI FLIPPER

Parameters	*Area*	*Weight*	a_1	*c*	α	β
Value	0.0036m^2	20g	15mm	30mm	120 °	130 °

IV. EXPERIMENTAL EVALUATION

After the structural parameters are determined by theoretical and simulation analysis, comparative experiments are designed to test the effect of bionic origami flippers on the swimming performance of the frog-inspired robot and verify the feasibility and practicability of its structure. The developed bidirectional adaptive flipper with an origami structure is assembled on the prototype of a frog-inspired swimming robot, as shown in Fig. 7a. The flipper has 4 segments with a radial length of 120 mm and an area of 3600 mm^2. A comparison with a straight plate flipper and an open-close flipper is shown in Fig. 7b.

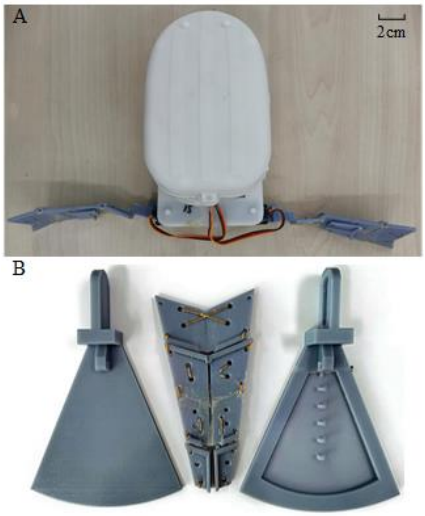

Fig. 7. The frog-inspired swimming robot and its different structural forms of flippers.

A. Translational swimming

The flippers can stretch, maintain and contract in water, and drive the frog-inspired swimming robot to move by remotely coordinating and controlling each driving motor. The experimental video is processed to obtain the swimming sequence of the robot with different flippers. The 'Start' in Fig. 8 is marked as the starting position of the robot, which is fixed, and the 'End' is marked as the end position of the robot. The shadow of the last figure represents the absolute position of the robot in the initial stage, which is also expressed in the subsequent action sequence diagram.

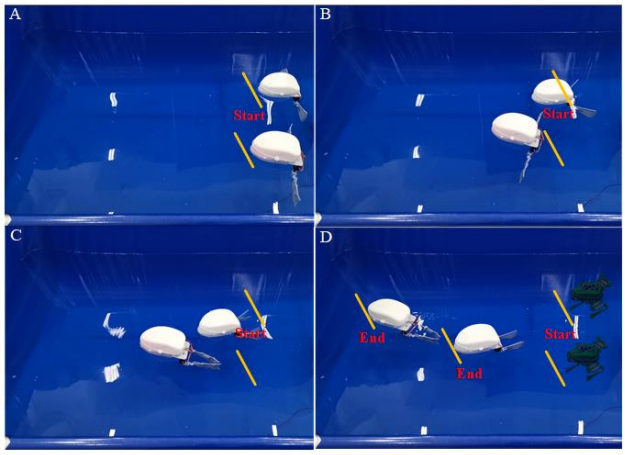

Fig. 8. Comparison of translational swimming sequences.

Due to the imbalance of the counterweight and the water flow disturbance caused by the movement of the two robots, the robot did not carry out strict linear propulsion motion, but this did not affect the result of the comparative experiment. The forward distance of the robot with open-close flippers is approximately 0.6 m, and the average propulsion speed is approximately 0.06 m/s. In contrast, the robot with the smaller origami flipper can reach a propulsion speed of 0.1 m under the same external environment, which is approximately twice as far as the former. The analysis of two groups of experimental results shows that the thrust generated by the flipper is enough to overcome the water resistance to make the robot move forward, but the motion efficiency of the origami flipper is relatively better. Although the open-close flipper can produce a one-way drainage mechanism to reduce the recovery resistance during the recovery motion, to ensure that the movable flipper can return to the initial position, it is necessary to overcome a certain spring resistance and water resistance, which leads to a short backward motion state of the robot. In contrast, the origami flippers swing softly under the action of water flow, and there is no obvious backward movement trend, which greatly improves the locomotion efficiency of the robot. To further test its swimming performance, we carried out the robot's countercurrent translational swimming experiment on this basis (see supplementary video). The average propulsion speed of the robot with the origami flippers is approximately 0.05 m/s. Although the speed is slightly slower than that in still water, it is still more efficient than the open-close flippers in the case of fluid motion, which preliminarily verifies the rationality of the bidirectional adaptive flipper structure design based on the origami principle.

B. Turning

The frog realizes the turning movement by generating a deflection torque through the asynchronous movement of the limbs. The same motion form is applied to the prototype of the robot with different flippers, and the motion sequence is shown in Fig. 9. Since the mass and volume of the robot are mainly concentrated on the torso, the water resistance of the robot during turning is high, which affects the rotation efficiency to a certain

extent. Compared with the open-close flipper, the origami flipper greatly reduces the recovery motion resistance of the robot. The rotation angle can reach 90° in two cycles, which is approximately twice that of traditional flippers, and the motion efficiency is obviously higher.

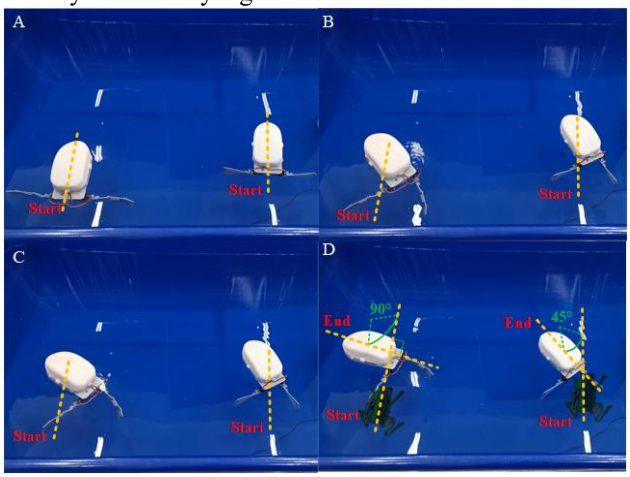

Fig. 9 Comparison of turning sequences.

C. Collision experiments

To test the structural strength of the flipper when it collides with the outside world and its influence on the movement, collision experiments on land and in water were carried out. It can be seen from the land experiment that the origami flippers have undergone adaptive deformation without damage when contacting objects, and the position of the torso has not changed. However, the open-close flipper can only drive the torso to shift because it cannot produce deformation. If the collision occurs at a faster speed at this time, the flipper is easily damaged. From the point of view of the effect of swimming in the water, compared with the slight changes caused by the use of origami flippers, the swimming trajectory of the open-close flippers changed by 45° , which was almost three times that of the former, further indicating the rationality of the origami flippers structure.

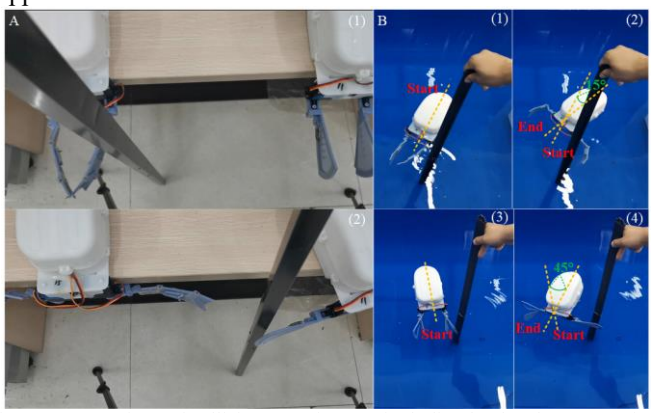

Fig. 10. Comparison of collision experiments, including land and water motion experiments.

D. Environmental adaptability experiment

On the basis of the collision experiment, an environmental adaptability experiment is carried out to further verify the motion performance of the origami flipper, and the motion sequence is shown in Fig. 11. Two frog-inspired swimming robots with origami (front) and open-close (rear) flippers swim along the wall of the swimming pool, and their motion trajectories are extracted and represented by green lines and red lines, respectively. It can be seen that due to the lack of self-adaptability in the open-close flipper, the left flipper and the pool wall contact and collide during the recovery movement, resulting in a force that causes the robot to move backwards, which greatly reduces the movement efficiency. However, the robot with the origami flipper does not exhibit the above situation and gradually moves forward with the help of the flipper. In particular, it should be noted that in the face of a 90° corner, the robot successfully adjusted the direction of motion after several swimming cycles and crossed the corner, while the robot with open-close flippers was trapped in the corner and could not be turned. The adaptive flipper with an origami structure has good compliance and can expand and contract independently along the crease under the action of water. Therefore, it can show good environmental adaptation compared with traditional non-shrinkable flippers.

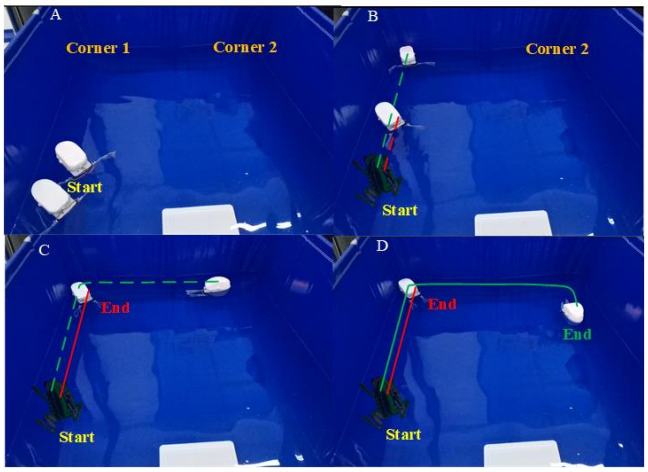

Fig. 11. Environmental adaptability experiment. The front and rear are frog-inspired swimming robots with origami and open-close flippers, respectively. Their corresponding locomotion trajectories are represented by green lines and red lines.

V. Discussion And Conclusion

The flipper is not only the propulsion unit for the frog-inspired swimming robot but also a source of resistance. Its structure and form have a great influence on the locomotion efficiency of the robot. To overcome the inability the existing flipper to adjust its structure according to the locomotion state, an adaptive flipper with an origami structure is proposed based on the structure analysis and swimming characteristics of a biological frog flipper. A theoretical deformation analysis model of the flipper is established by the self-defined folding coefficient. Combined with the analysis of the flow field information during the simulation locomotion, the structural parameters of the flipper are determined with the goal of maximizing the driving torque provided during the propulsion process, and then the bionic origami flipper is prepared by integrating 3D printing and bonding. The flipper combines the characteristics of rigid, soft and soft materials and does not require additional device drive during propulsion and recovery motion, which makes the robot's structure simpler and lighter.

IEEE Robotics and Automation Letters (RA-L) paper, presented at ICRA 2024, Yokohama, Japan. Cite as RA-L paper.

The linear locomotion experiment shows that the robot can move forward at an average speed of 0.1 m/s, which is twice the moving distance of the robot with an open-close flipper, and there is no obvious trend of backward movement in the recovery process. Its turning locomotion is also more flexible and can reach 90° in two cycles. The collision experiment and the successful crossing of the corner show that the flipper can contract along the crease during movement, indicating that the flipper has good environmental adaptability, which verifies the feasibility and rationality of the designed structure.

Although the performance of this bionic flipper has been improved, it still cannot achieve the full effect of real flippers. Therefore, designing a new structure with the help of the biological prototype and controlling its contraction and extension by stimulating muscles will further improve the bionics and intelligence of the robot.[36] It is believed that this is a development trends for bionic robots in the future.

VI. Author Disclosure Statement

No competing financial interests exist.

VII. Acknowledgement

This work is supported by the National Natural Science Foundation of China (Grant No. 51675124). The authors are very grateful to the editors and reviewers for their valuable comments, which improved the paper.

References

[1] B. X. Zhu, F. S. Yu, W. Liang, et al. Analysis of underwater vehicle structure and its development trend. *Ship Engineering*, 42 (2): 1-7+84, 2020.

[2] J. W. Zhang, F. S. Yu, Z. L. Jun, et al. Application status and development trend of underwater propulsion form.*Ship Engineering*,43 (6): 61-65+78, 2021.

[3] R. Baines, S. K. Patiballa, J. Booth, et al. Multi-environment robotic transitions through adaptive morphogenesis. *Natur*e, 610(7931): 283-289, 2022.

[4] T. M. Wang, X. B. Yang, J. H. Liang.Summarization of the development status of bionic autonomous underwater robots with central fin / opposite fin propulsion mode.*Robot*, 35 (3) : 352-362+384, 2013.

[5] Y. Yang, G. Zhou, J. Q. Zhang, et al. Design, modeling and control of a novel amphibious robot with dual-swing-legs propulsion mechanism. *IEEE/RSJ International Conference on Intelligent Robots and Systems (IROS)*, pp. 559-566, 2015.

[6] J. Zhang, J. Zhou, S. Yuan, et al. Motion mechanism and thrust characteristics of amphibious robots with long fin fluctuation for propulsion on hard level ground. *Bioinspiration & Biomimetics*, 17(5): 056006, 2022.

[7] Y. R. Xu, P. C. Li.Trends in the development of underwater robots. *Nature*,33 (3) : 125-132 + 2, 2011.

[8] S. Q. Wang, J. Z. Fan, G. F. Liu. Research status and development trend of frog-inspired robots. *Robotica*,:1–21, 2023.

[9] W. Zhang, J. Z. Fan, Y. H. Zhu, et al. A Method for Mechanism Analysis of Frog Swimming Based on Motion Observation Experiments. *Advances in Mechanical Engineering*, 1–13, 2014.

[10] Y. Tang, L. Qin, X. Li, et al. A frog-inspired swimming robot based on dielectric elastomer actuators. *IEEE/RSJ International Conference on Intelligent Robots and Systems (IROS)*, pp. 2403-2408, 2017.

[11] J. Z. Fan, Y. L. Qiu, W. Zhang, et al. Dynamics analysis of frog-like swimming robot. *Mechanical design and manufacturing*, (1) : 4, 2015.

[12] J. Z. Gul, K. H. Kim, J. H. Lim, et al. FSI modeling of frog inspired soft robot embedded with ALD encapsulated flex sensor for underwater synchronous swim. *IEEE International Symposium on Robotics and Intelligent Sensors (IRIS)*, pp. 255-259, 2017.

[13] J. Z. Fan, Y. L. Qiu, W. Zhang, et al. Mechanism design of bionic frog swimming robot. *Robot*,37 (2) : 9, 2015.

[14] J. Pandey, N. S. Reddy, R. Ray, et al. Multi-body dynamics of a swimming frog: A co-simulation approach. *IEEE International Conference on Robotics and Biomimetics (ROBIO)*, pp. 842-847, 2013.

[15] W. Zhang, J. Z. Fan, H. G. Cai. Design of a novel frog-inspired hopping leg. *IEEE International Conference on Information and Automation*, pp. 277-282, 2017.

[16] J. Z. Fan, P. C. Kong, B . W. Yuan, et al. Optimization of a frog inspired robot powered by pneumatic muscles. *IEEE International Conference on Mechatronics and Automation (ICMA)*, pp. 602-607, 2017.

[17] J. Z. Fan, B . W. Yuan, Q. L. Du, et al. Joint Design and Position Servo Control of Frog Inspired Robot Based on Pneumatic Muscle and Reset Spring. *IEEE International Conference on Mechatronics and Automation (ICMA)*, 2018.

[18] J. Z. Fan, P. C. Kong, W. Zhang.Structural design of pneumatic muscle-driven bionic frog swimming robot. *Journal of Harbin University of Commerce: Natural Science Edition*,32 (5): 6, 2016.

[19] J. Pandey, N. S. Reddy, R. Ray, et al. Biological Swimming Mechanism Analysis and Design of Robotic Frog. *IEEE International Conference on Mechatronics and Automation, Takamatsu*, pp. 1726-1731, 2013

[20] J. Z. Fan, W. Zhang, P. C. Kong, et al. Design and Dynamic Model of a Frog-inspired Swimming Robot Powered by Pneumatic Muscles. *Chinese Journal of Mechanical Engineering*, 30(5): 1123-1132, 2017.

[21] J. Z. Fan, S. Q. Wang, Q. G. Yu, et al. Swimming Performance of the Frog-Inspired Soft Robot. *Soft Robotics*, 7(5): 615-626, 2020.

[22] Q. J. Ze, S. Wu, J. Z. Dai, et al. Spinning-enabled wireless amphibious origami millirobot. *Nature Communications*, 13(1): 3118, 2022.

[23] H. Yasuda, K. Johnson, V. Arroyos, et al. Leaf-Like Origami with Bistability for Self-Adaptive Grasping Motions. *Soft Robotics*, 9(5): 938-947, 2022.

[24] Q. Chen, F. Feng, P. Lv, et al. Origami Spring-Inspired Shape Morphing for Flexible Robotics. *Soft Robotics*, 9(4): 798-806, 2022.

[25] J. Zou, Y. Lin, C. Ji, et al. A Reconfigurable Omnidirectional Soft Robot Based on Caterpillar Locomotion. *Soft Robotics*, 5(2): 164-174, 2018.

[26] S. Wu, Q.J. Ze, J. Dai, et al. Stretchable origami robotic arm with omnidirectional bending and twisting. *Proceedings of the National Academy of Sciences*, 118(36): e2110023118, 2021.

[27] S. Zhang, X. Ke, Q. Jiang, et al. Programmable and reprocessable multifunctional elastomeric sheets for soft origami robots. *Science Robotics*, 6(53): eabd6107, 2021.

[28] J. G. Lee, H. Rodrigue. Origami-Based Vacuum Pneumatic Artificial Muscles with Large Contraction Ratios. *Soft Robotics*, 6(1): 109-117, 2019.

[29] S. Mintchev, J. Shintake, D. Floreano. Bioinspired dual-stiffness origami. *Science Robotics*, 3(20): eaau0275, 2018.

[30] L. Paez, G. Agarwal, J. Paik. Design and Analysis of a Soft Pneumatic Actuator with Origami Shell Reinforcement. *Soft Robotics*, 3(3): 109-119, 2016.

[31] J. Cai, Z. Ren, Y. Ding, et al. Deployment simulation of foldable origami membrane structures. *Aerospace Science and Technology*, 67: 343-353, 2017.

[32] C. M. Wheeler, M. L. Culpepper. Soft Origami: Classification, Constraint, and Actuation of Highly Compliant Origami Structures. *Journal of Mechanisms and Robotics*, 8(5): 051012, 2016.

[33] D. Rus, M. T. Tolley. Design, fabrication and control of origami robots. Nature Reviews Materials, 3(6): 101-112, 2018.

[34] Q. J. Ze, S. Wu, J. Jun, et al.Soft robotic origami crawler. *Science advance*, 8, eabm7834, 2022.

[35] D. S. Shah, J. P. Powers, L. G. Tilton, et al. A soft robot that adapts to environments through shape change. *Nature Machine Intelligence*, 3(1):51-59, 2020.

[36] T. Thang Vo-Doan V. Than Dung and H. Sato. A Cyborg Insect Reveals a Function of a Muscle in Free Flight. *Cyborg Bionic Syst*. 2022;